Final version is available on: https://doi.org/10.1115/1.4050214

Evaluation of optical transmissivity of transparent materials on the performance of solar flat plate collectors

Saboor Shaik[a], Manvendra Bhardwaj[a], Somya Agarwal[a], Raja Sekhar Y[a,]* Md. Hasanuzzaman[b]

K V Sharma[c]

[a] Department of Thermal and Energy, School of Mechanical Engineering, Vellore Institute of Technology, Vellore, Tamil Nadu, India 632014.

[b] UM Power Energy Dedicated Advanced Centre (UMPEDAC), Level 4, Wisma R&D, University of Malaya, 59990 Kuala Lumpur, W.Persekutuan Kuala Lumpur, Malaysia

[c] Centre for Energy Studies, JNTUH College of Engineering, JNTU Hyderabad, Kukatpally, Hyderabad, India 500085

*Corresponding author: rajasekhar.y@vit.ac.in

The energy gain of domestic solar water heating systems is determined by solar to thermal energy conversion and optical efficiency of glazing. For this study, solar transmission properties of different transparent glazing materials such as acrylic, low-, medium-, and high-iron glasses were measured. The thermal efficiency of the collector under natural convection mode was compared for different transparent covers determined by numerical simulation using the Hottel-Whillier-Bliss equation. The low-iron glass (LiG-12 mm) has 16.3% and 20% higher thermal efficiency than medium (MiG-12 mm) and high iron glasses (HiG- 12 mm), respectively, for a peak summer day. The effect of glass thickness on thermal performance is noteworthy in glasses than in acrylic glass sheets. Low-iron content glass with 6 mm thickness has the highest thermal and optical efficiency of 63.2% and 75.65%, respectively, for the optimum tilt of the collector for Vellore city in Tamilnadu, India. The results are useful in the selection of glass covers for energy-efficient solar flat plate collectors.

1. Introduction:

The solar flat plate collectors are widely employed for collecting the incident solar radiation and they can heat the working fluid to a temperature range of 70-100°C based on the collector design [1,2]. Collectors with sun tracking systems can enhance thermal performance but they are not always applicable due to their additional material and operational costs [3]. The solar flat plate collector (SFPC) performance mainly depends on local meteorological conditions, incident solar radiation, collector orientation, tilt angles, absorber, and cover materials [4,5]. The three major parts of SFPC are absorber plate, glazing, and insulation. The absorber plate absorbs solar radiation and transmits it to the working fluid, the glazing traps the short-wave radiation, and insulation prevents the heat losses [6]. Glazing is the top cover of SFPC and it has three major purposes: to diminish convective and radiative losses from the absorber, to allow solar radiation to absorber plate, and to protect the absorber plate from the environment [7]. Glass and plastics are commonly used materials to glaze solar flat plate collectors. Glasses transmit the maximum amount of short-wave radiation and plastics transmit both short-wave and long-wave radiations. The plastics are strong, lightweight, and low-cost materials but they can not withstand high temperatures like glasses [8]. The side and bottom ends of SFPC are usually well insulated but the major heat losses occur from the glass cover [9]. Therefore, SFPC's thermal performance also depends on the glass cover material and its thickness. In this technical brief, the thermal

Final version is available on: https://doi.org/10.1115/1.4050214

performance of SFPC has been analyzed considering the optical characteristics of the twelve glazing types of various thicknesses (acrylic, low-, medium-, and high-iron glasses) for Vellore (12.91° N, 79.13° E) in Tamilnadu, India. For this purpose, the spectral characteristics of the transparent materials were measured using a spectrophotometer and solar optical properties of glazing materials were utilized to estimate thermal and optical efficiencies of SFPC.

2. Materials and methods

The transparent acrylic, as well as glass samples having various thicknesses chosen for this study. The acrylic sheets and glasses were procured from Padmavathi Glass- Saint Gobain dealers, Vellore, Tamilnadu, India. The four different thicknesses of Acrylic glass sheets are termed as AGS- 4mm, AGS- 5mm, AGS- 6mm, and AGS- 8mm along with three different thicknesses of low-iron glass, namely LiG- 6mm, LiG- 8mm, and LiG- 12mm were selected. Similarly, one medium-iron glass, namely MiG- 12mm, and four high-iron glass samples termed as HiG- 4mm, HiG- 6mm, HiG- 8mm, and HiG- 12mm were considered. Fig. 1a shows the photograph of different types of transparent materials considered.

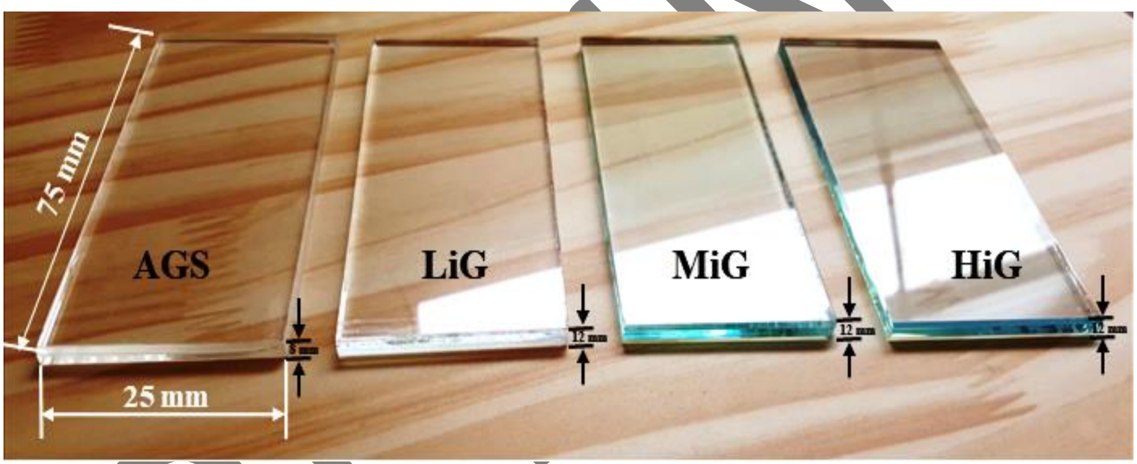

(a)

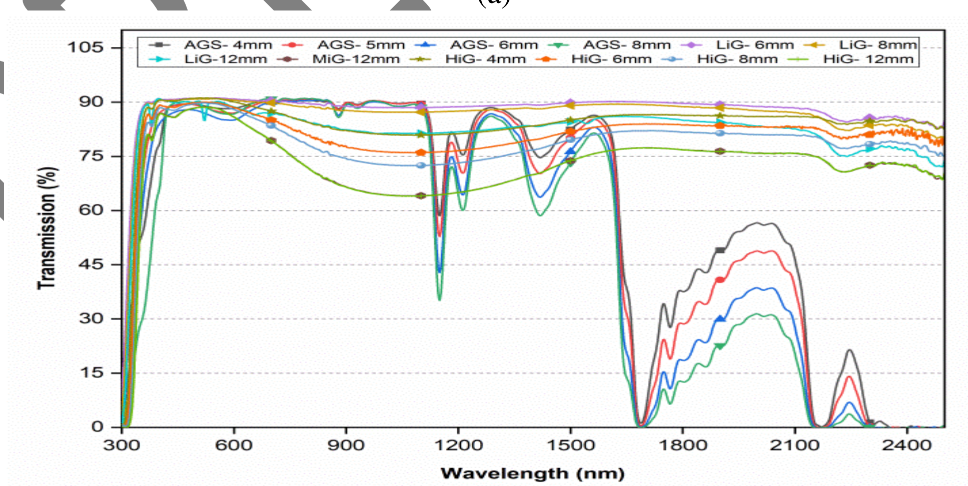

(b)

Fig. 1. a.) Glass cover samples b.) Spectral transmission of SFPC glass covers

Final version is available on: https://doi.org/10.1115/1.4050214

The transparent samples were characterized to determine transmission for different wavelengths using Lambda 950 UV/Vis/NIR spectrophotometer. The spectral transmission data of glass covers were further deduced to obtain solar transmittance using a weighted average method as per British Standard European Norm 410 [10,11]. Experiments were conducted to explore spectral properties of various glass covers of AGS, LiG, MiG, and HiG using a spectrophotometer in the solar spectrum range 300-2500 nm as depicted in Fig. 1(b). The spectrophotometer has a wavelength accuracy of ± 0.08 nm in the Ultraviolet-Visible region and ± 0.30 nm in the Near-Infrared region. The instrument works on the principle of double-beam, double monochromatic, ratio recording spectrophotometer. The detectors used in the systems have photomultiplier and peltier controlled lead sulfide (PbS) for UV/Vis and NIR wavelength range, respectively.

Eq. (1) was used to obtain solar transmittance of twelve glass covers of solar flat plate collector where Sλ is the relative spectral distribution of the solar radiation, Δλ is wavelength interval (2 nm), and (λ) is spectral transmission wavelength obtained from the spectrophotometer.

$$T = \sum_{\lambda=300\text{nm}}^{\lambda=2500\text{nm}} S_\lambda \, \tau(\lambda)\Delta\lambda \Bigg/ \sum_{\lambda=300\text{nm}}^{\lambda=2500\text{nm}} S_\lambda \, \Delta\lambda \qquad (1)$$

3. Design and Analytical methodology

The SFPC is designed in Vellore city, and it is assumed to be fixed in one position year-around without sun tracking. Vellore falls under the hot and dry climatic zone and has peak summer on April 21st and winter on December 21st; The solar radiation incident on a tilted surface can be calculated from Eq. (2) [12]. In this Eq. (2), A, B, and C are solar radiation in the absence of atmosphere (W/m^2), atmospheric extinction coefficient, sky radiation coefficient, respectively. β is a solar altitude angle. θ is an incidence angle, The value of k is 0^o for the vertical surface, and k= 90^o for the horizontal surface. For a collector tilt angle of 10^o, the value of k would be 80^o. The albedo was represented by $\rho_{g,}$ and it is considered as 0.2.

$$I=\left(\frac{A}{\exp(B/\sin\beta)}\cos(\beta)\cos(\gamma)\cos(k)-\sin(\beta)\sin(k)\right)+C1.\frac{A}{\exp(B/\sin\beta)}.\left(\frac{1+\mathrm{Sin}(k)}{2}\right)+(C1+\sin\beta)\frac{A}{\exp(B/\sin\beta)}\rho_g\left(\frac{1-\mathrm{Sin}(k)}{2}\right) \qquad (2)$$

The design parameters of the SFPC are presented in Fig. 2. The analysis was carried out for peak summer and winter days at Vellore to arrive at optimum collector tilt (11.5^o) and orientation (south) for year-around maximum incident solar flux. Table 1 shows the various parameters considered for the thermal analysis of a flat plate collector. The thermal performance of the collector can be investigated by the parameters such as collector efficiency factor (F'), heat removal factor (F_R), useful heat flux (Q_u), thermal efficiency (η_T), and optical efficiency (η_{Opt}). The values are obtained with Eqs. (3)-(7) [13,14]. In Eq. (4), The values of F_R and overall loss coefficient (U_l) cannot be directly computed as the value of one is dependent on the other.

Final version is available on: https://doi.org/10.1115/1.4050214

Therefore, an iterative procedure is followed. For the first iteration, U_l has been assumed as 4 W/m^{2}K and it is a reasonable assumption for a collector with a glass cover [13]. Eq. (5) is called the Hottel-Whillier-Bliss equation which is used to calculate useful energy gain when the inlet fluid temperature is known. S denotes the incident radiation absorbed by the absorber plate and estimated as a product of incident flux (I) and transmissivity-absorptivity product, τα, and Φ is absorber plate effectiveness.

$$F' = \frac{1}{W.U_l\left[\frac{1}{U_l[(W-D_o)\phi + D_o]} + \frac{1}{\pi.D_i.h_f}\right]} \quad (3)$$

$$F_R = \frac{\dot{m}C_p}{U_l A_p}\left[1 - \exp\left(-\frac{F' U_l A_p}{\dot{m}C_p}\right)\right] \quad (4)$$

$$Q_u = F_R.\alpha.\tau.I.A_p - F_R.U_l.A_p\ .(T_{fi} - T_a) \quad (5)$$

$$\eta_T = F_R.\alpha.\tau - F_R.U_l.\frac{(T_{fi} - T_a)}{I} \quad (6)$$

$$\eta_{Opt} = S/I \quad (7)$$

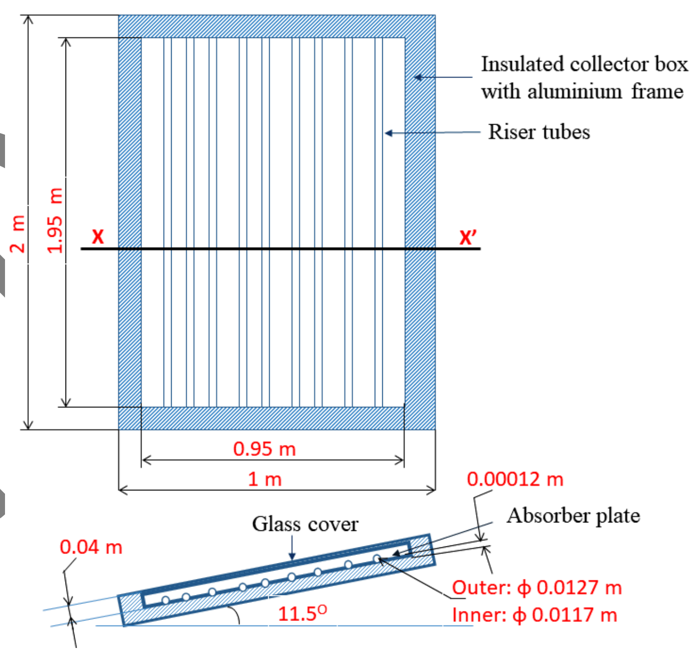

Fig. 2. Schematic of SFPC

Final version is available on: https://doi.org/10.1115/1.4050214

Table 1 Parameters considered

Parameter	Specification
Location and solar parameters:	
Location of collector	Vellore: 12.9165°N, 79.1325°E
Solar parameters [12]: A (W/m^2), B & C (Dimensionless) Peak summer: April 21st A, B, and C value Peak winter: December 21st A, B, and C value	613.35, 0.121, and 0.395 622.52, 0.000, and 0.243
Collector design parameters:	
Collector area (Ac) (Length x Width) (m^2)	2 x 1
Absorber area (Ap) (Length x Width) (m^2)	1.95 x 0.95
No of tubes (N)	9
Collector tilt (k) (deg)	11.5°
Thermal conductivity of plate material (kp) W/mK	350
Absorber plate thickness (δp) (m)	0.0012
Diameter of tube (outer (Do), inner (Di)) (m)	0.0127, 0.0117
Wind speed (v) (m/s)	2.5
Spacing between glazing cover and absorber (L) (m)	0.04
Emissivity of collector plate (εc)	0.85
Emissivity of absorber plate (εp)	0.14
Absorptivity (α)	0.85
Pitch (W) (m)	0.105
Fluid to tube heat transfer coefficient (hf) (W/m^2K)	205
Surface azimuth angle (γ) (deg)	0° (South oriented)
Glazing size and their optical properties:	
Sample size for spectrophotometer (Length x Width) (m^2)	0.02 x 0.01
Solar Transmittance (τ) $AGS_{4,5,6,8\ mm}$ $LiG_{6,8,12\ mm}$ $MiG_{12\ mm}$ $HiG_{4,6,8,12\ mm}$	 0.78, 0.77, 0.75, and 0.74 0.89, 0.88, and 0.84 0.73 0.82, 0.81, 0.79 and 0.71

4. Results and discussions

The performance of the collector in terms of useful heat flux and collector efficiency factor for LiG- 6mm is depicted in Fig. 3. The results show the availability of useful heat flux at 7 am (LAT) in the morning during a peak summer day, whereas it is zero during the peak winter day. The mass flow rate varying between 0.01 to 0.02 kg/s, has a significant influence on useful heat absorbed during the diurnal time. In contrast, 0.025 kg/s mass flow rate was observed to be insignificant. This is due to the reduction in difference of inlet and outlet fluid temperature with the increased flow rates [15].

Final version is available on: https://doi.org/10.1115/1.4050214

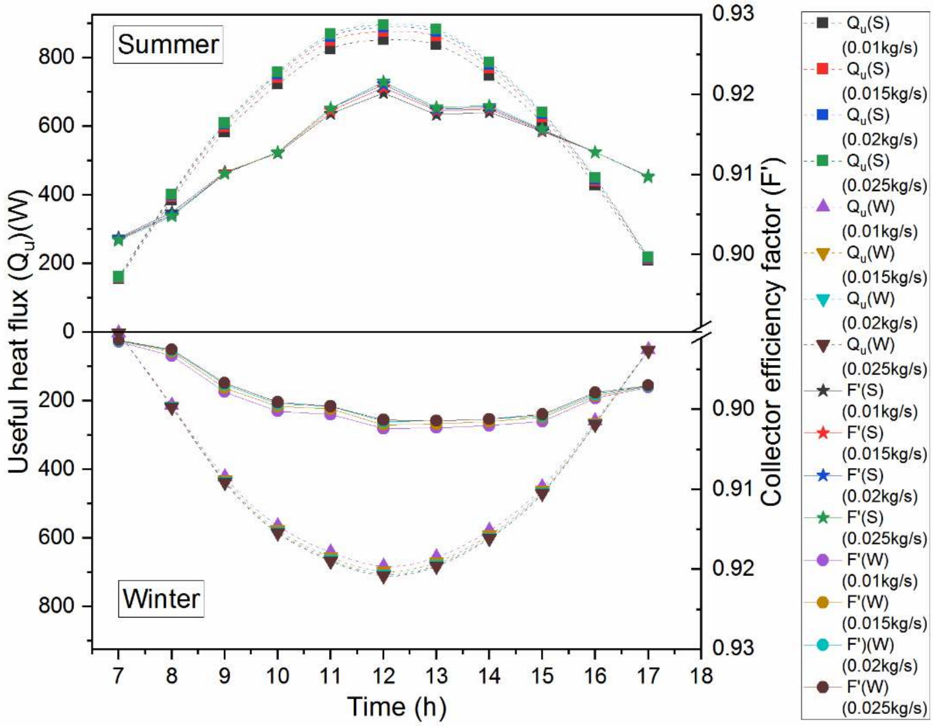

Fig. 3. Useful heat flux and collector efficiency factor at various mass flow rates for LiG-6mm

Fig. 4. depicts the useful heat flux and collector efficiency factor at the mass flow rate of 0.02 kg/s for various glass covers of SFPC. LiG-6mm has the maximum value, whereas HiG-12mm has the least value on peak winter and summer days.

Final version is available on: https://doi.org/10.1115/1.4050214

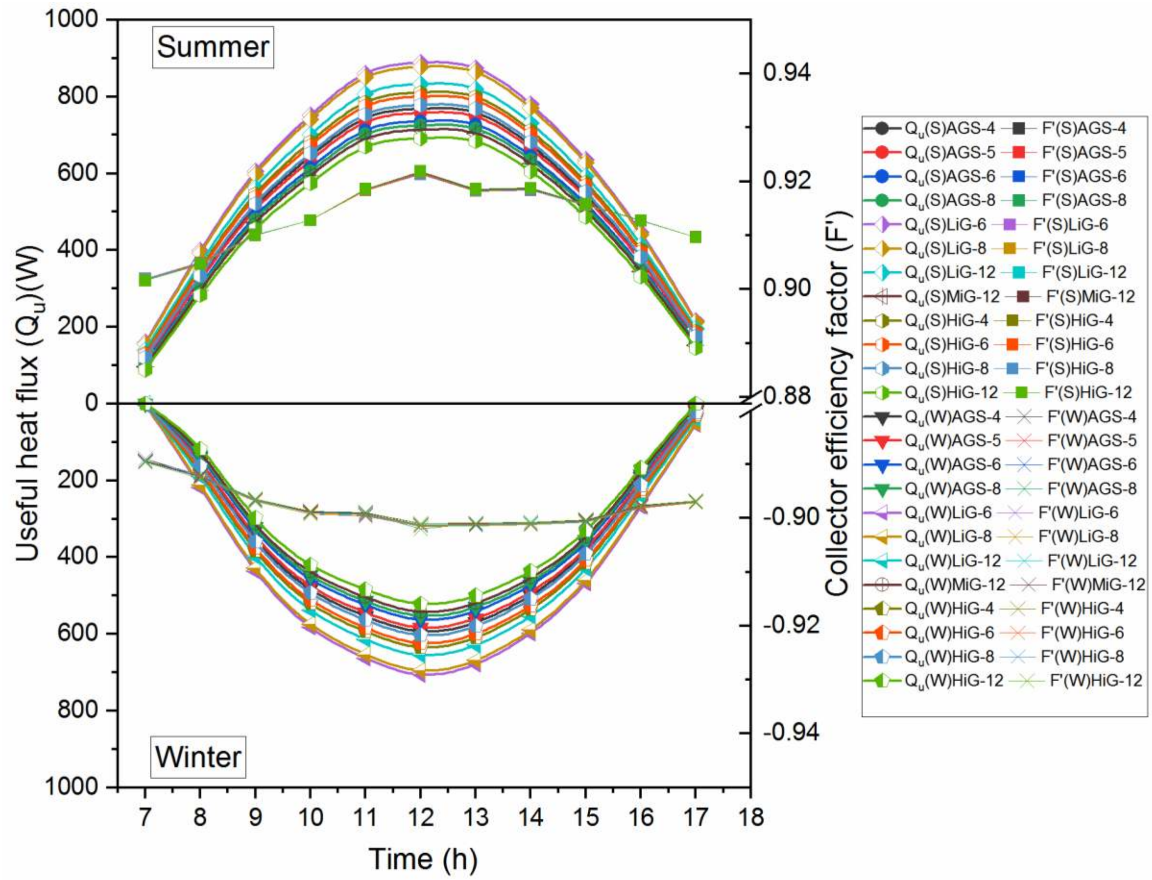

Fig. 4. Useful heat flux and collector efficiency factor at 0.02 kg/s mass flow rate for various glass covers of SFPC

Fig. 5. shows the relationship between ambient temperature and heat removal factor of SFPC with LiG-6mm at various mass flow rates. The results show that the heat removal factor of SFPC with LiG-6mm is influenced by ambient temperature, mass flow rate, and diurnal hourly radiation on peak summer and winter days. The maximum heat removal factor was obtained at noon (LAT), and the heat removal factor was the least at 7 am (LAT). The change in the heat removal factor is optimal in the mass flow rate range of 0.01-0.02 kg/s and remains unaltered at mass flow rates up to 0.025 kg/s.

Final version is available on: https://doi.org/10.1115/1.4050214

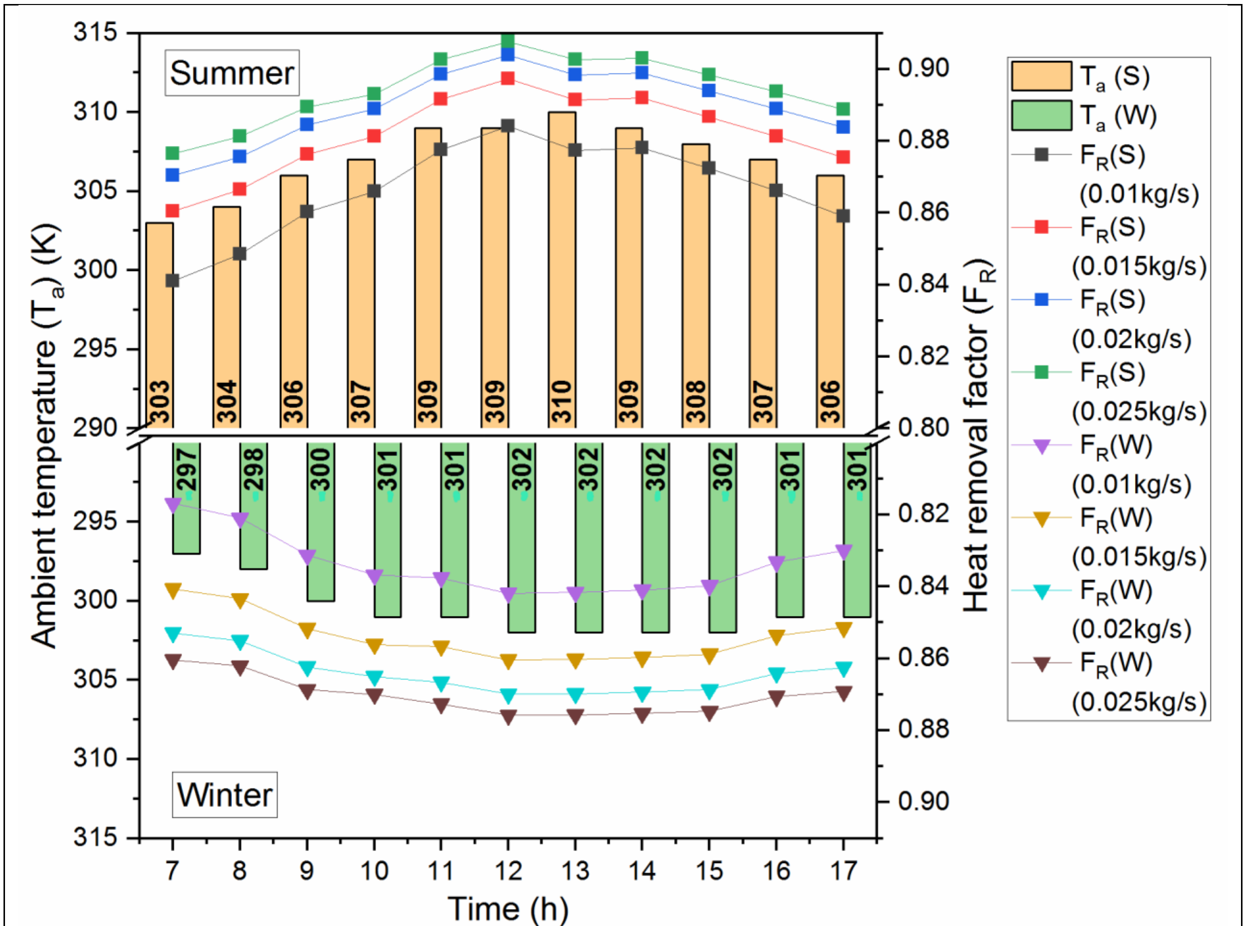

Fig. 5. Ambient temperature and heat removal factor at various mass flow rates and diurnal hours for LiG-6mm

Fig. 6. presents the heat removal factor and optical efficiency of glass covers at 0.02 kg/s mass flow rate. The results show that the thickness and the type of glass cover significantly influence the optical efficiency of the SFPC. It can also be observed that acrylic-based samples have lower optical efficiency than glass samples of the same thicknesses due to light absorption within its thickness. The optical efficiency of LiG- 6mm is 9.8% higher than the HiG- 6mm. The iron content of glass and its thickness significantly enhance the optical efficiency of SFPC. The low-iron glass (LiG-12 mm) has 14.97% and 18.21% higher optical efficiency than medium (MiG-12 mm) and high iron glasses (HiG- 12 mm), respectively. The optical efficiency order of preference for acrylic and glass covers is LiG- 6mm, LiG- 8mm, LiG- 12mm, HiG- 4mm, HiG- 6mm, HiG- 8mm, AGS- 4mm, AGS- 5mm, AGS- 6mm, AGS- 8mm, MIG- 12mm, and HiG- 12mm.

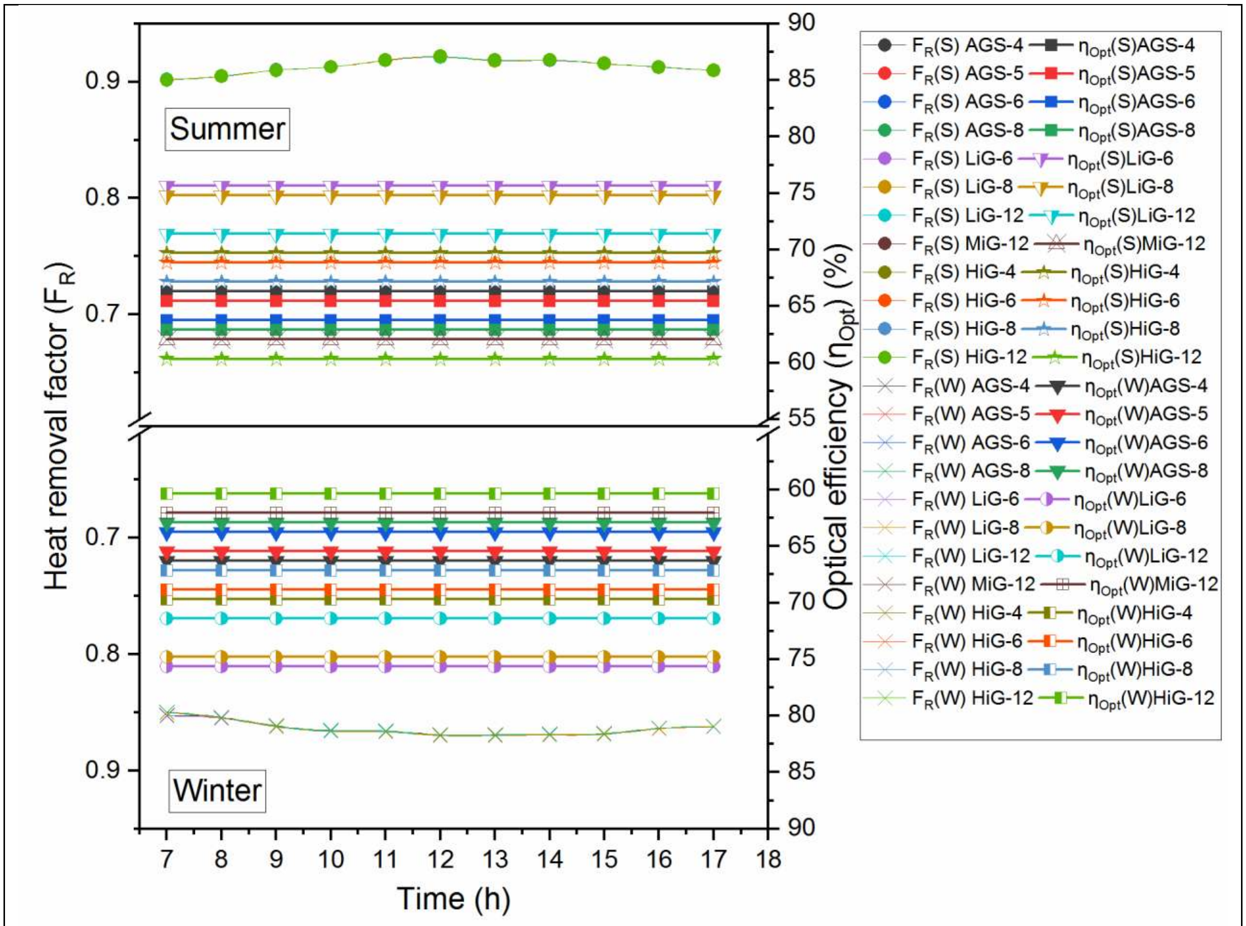

Fig. 6. Heat removal factor and optical efficiency at 0.02 kg/s mass flow rate for various glass covers of SFPC

Fig. 7. depicts the relationship between incident solar radiation and thermal efficiency at various mass flow rates and diurnal hours for SFPC of LiG-6mm. At 7 am (LAT) of the peak summer day, the thermal efficiency of the SFPC is higher than peak winter day. The thermal efficiency of SFPC follows a parabolic profile where an increase in thermal efficiency is significant for the mass flow rate up to 0.02 kg/s. After 0.02 kg/s mass flow rate, the increase in the thermal efficiency of SFPC is gradual.

Final version is available on: https://doi.org/10.1115/1.4050214

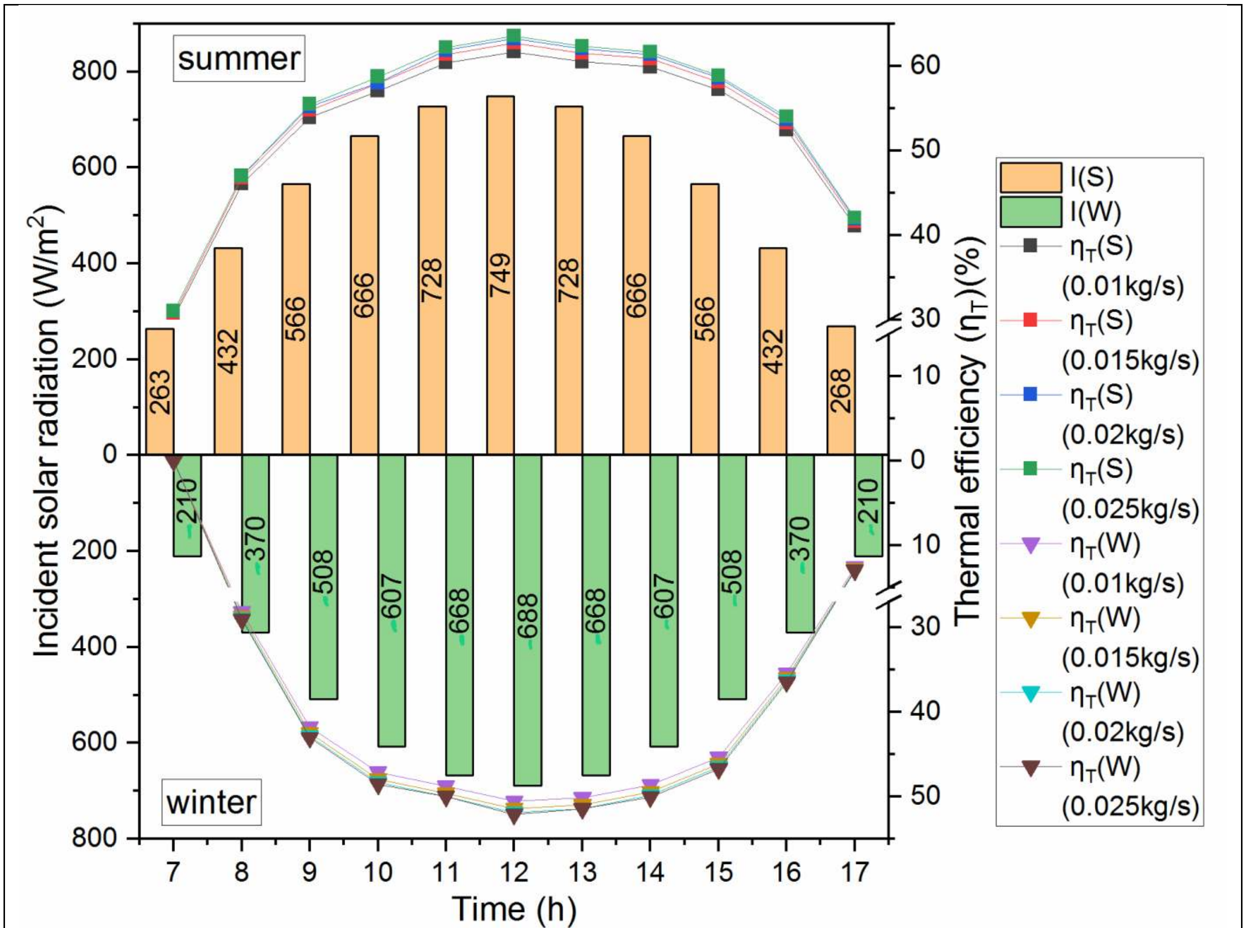

Fig. 7 Incident solar radiation and thermal efficiency at various mass flow rates and diurnal hours for LiG-6mm

Fig. 8. presents thermal efficiency variation for various glazing covers at 0.02 kg/s mass flow rate. SFPC with LiG-6mm was observed to be the most energy-efficient due to its highest thermal efficiency of 63.22% at solar noon on a peak summer day, followed by LiG-8mm (62.46%). The peak thermal efficiency of acrylic glazing on a peak summer day is limited to 54.89 % for lower thickness (4mm). The thermal efficiency of LiG- 6mm is 10.7% higher than the HiG- 6mm (ordinary clear glass). The low-iron glass (LiG-12 mm) has 16.3% and 20% higher thermal efficiency than medium (MiG-12 mm) and high iron glasses (HiG- 12 mm), respectively, during solar noon of a peak summer day.

Final version is available on: https://doi.org/10.1115/1.4050214

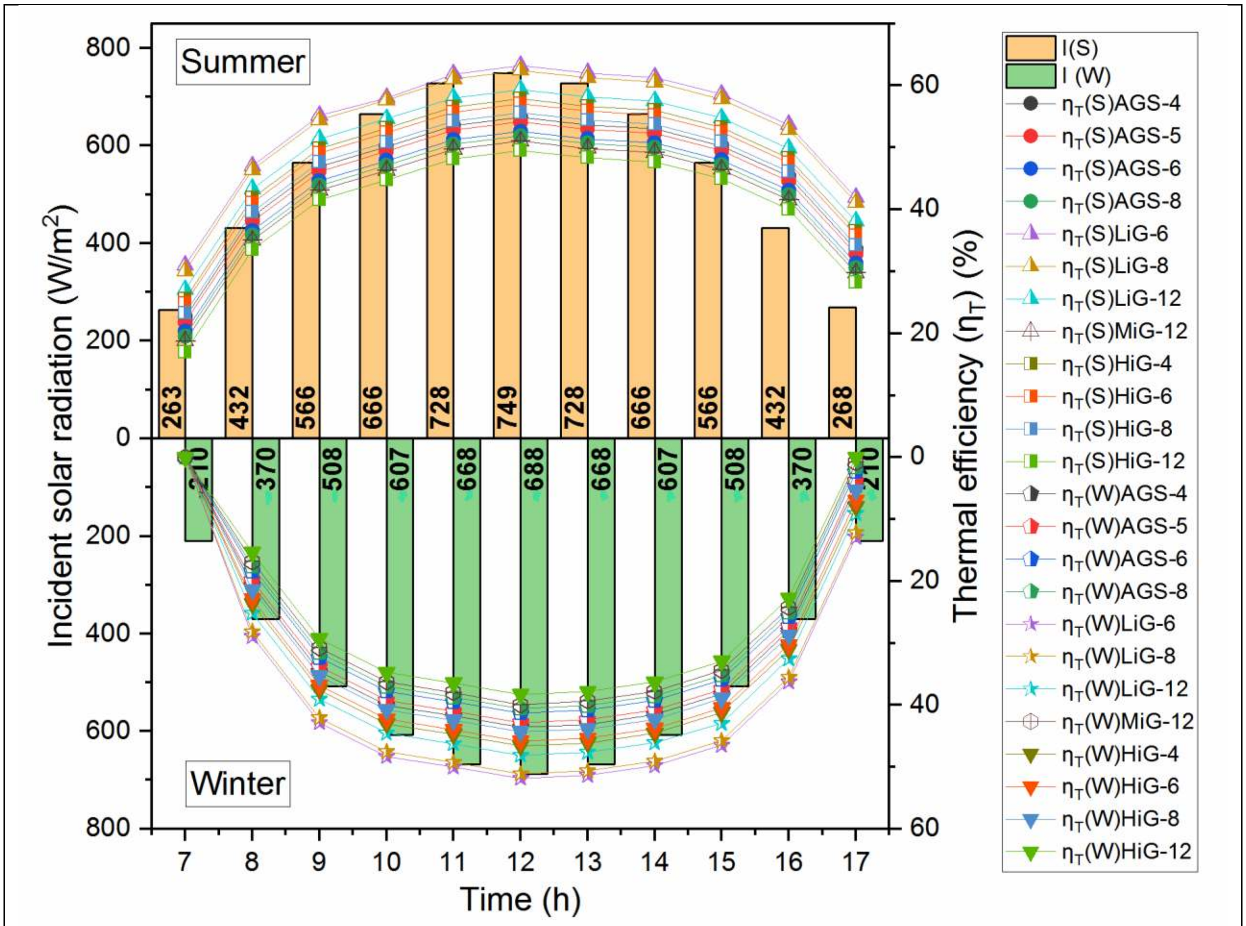

Fig. 8. Incident solar radiation and thermal efficiency at 0.02 kg/s mass flow rate for various glass covers of SFPC

5. Conclusion

Solar transmission is a crucial optical parameter of the glass cover that significantly affects the thermal and optical efficiencies of the SFPC. The acrylic glass sheet has shown better spectral transmission in the UV-VIS region. However, its spectral transmission is shallow in the NIR region compared to the glass. Glass is observed to be the best compared with acrylic glass due to its better solar transmission in both UV-VIS and NIR regions for enhancing solar influx absorbed by the absorber plate. The iron content of glass and its thickness play a significant role in enhancing thermal and optical efficiency. The low-iron glass (LiG-12 mm) has 16.3% and 20% greater thermal efficiency than medium (MiG-12 mm) and high iron glass (HiG- 12 mm), respectively, at noon on a peak summer day. The effect of glass thickness on thermal performance is noteworthy in glasses than in acrylic glass sheets. Low iron glass (LiG-6 mm) was observed to be the best due to its highest thermal (63.2%) and optical (75.65%) efficiencies, among the glass cover materials considered at an optimum inclination angle of the collector for Vellore in Tamil Nadu, India. The effect of the mass flow rate for a peak winter day is the lowest as compared to a peak summer day. So, it is concluded that for summer days, the collector must

Final version is available on: https://doi.org/10.1115/1.4050214

be operated at higher mass flow rates to gain maximum energy efficiency. The collector must be operated at a moderate mass flow rate during winter for reducing the pumping energy. The results of this work help the designers to select materials and operating parameters based on climatic conditions.

References

[1] F. Struckmann, "Analysis of flat—plate solar collector, Project Report MVK160, Heat and Mass Transport, Lund, Sweden, (2008).

[2] Y. Raja Sekhar, K. V. Sharma, M. Basaveswara Rao, Evaluation of Heat Loss Coefficients In Solar Flat Plate Collectors, Journal of Engineering and Applied Sciences, 4 (5) (2009) 15-19.

[3] M. Lave, J. Kleissl, Optimum fixed orientations and benefits of tracking for capturing solar radiation in the continental United States, Renewable Energy, 36 (3) (2011) 1145-1152.

[4] Y. Kashyap, A. Singh, Y. Raja Sekhar, Exergy Analysis of a Flat Plate Solar Collector With Grooved Absorber Tube Configuration Using Aqueous ZnO–Ethylene Glycol. ASME. J. Sol. Energy Eng. 140 (6) (2018) 061011.

[5] C. Stanciu, D. Stanciu, Optimum tilt angle for flat plate collectors all over the World – A declination dependence formula and comparisons of three solar radiation models, Energy Conversion and Management 81 (2014) 133–143

[6] R. Bakari, R.J. Minja, K. N. Njau, Effect of glass thickness on performance of flat plate solar collectors for fruits drying, Journal of energy, (2014) 1-8.

[7] F. DeWinter, Solar Collectors, Energy Storage, and Materials, MIT Press, (1990).

[8] I. V. Ion, J. G. Martins, Design, Developing and Testing of a Solar Air Collector, Glass, University of Minho, (2006).

[9] M. Khoukhi, S. Maruyama, Theoretical approach of a flatplate solar collector taking into account the absorption and emission within glass cover layer, Solar Energy, 80, (7) (2006) 787–794.

[10] ASTM E424, Test for solar energy transmittance and reflectance (terrestrial) of sheet materials, Washington DC, USA, (1971) 1320-1326.

[11] BS EN 410, Glass in Building-Determination of luminous and solar characteristics of the glazing, British Standards, (1998). 1-24.

[12] J.A. Duffie, W.A. Beckman, Solar engineering of thermal processes, Wiley, New York (1980).

[13] Sukhatme, P. Suhas, J. K. Nayak. Principles of thermal collection and storage. Solar Energy, 3rd Edition, Tata McGraw Hill Publishing company, New Delhi (1996).

[14] B. Kalidasan, T. Srinivas. Study on Effect of Number of Transparent Covers and Refractive Index on Performance of Solar Water Heater. Journal of Renewable Energy (2014).

[15] S.K. Verma, A.K. Tiwari, D.S. Chauhan. Performance augmentation in flat plate solar collector using MgO/water nanofluid. Energy conversion and management, 124 (2016) 607-617.